

Saturation in central-forward jet production in p-Pb collisions at LHC *

SEBASTIAN SAPETA

Institute for Particle Physics Phenomenology,
Durham University, South Rd, Durham DH1 3LE, UK

We show that saturation can manifest itself in central-forward dijet production in p-A collisions. In spite of large transverse momenta of the jets, the almost back-to-back dijet configurations are able to probe gluon density at low x and low k_t . We perform our study in the framework of high energy factorization with the unintegrated gluon density given by a nonlinear QCD evolution equation. We show that the formalism can successfully account for features measured in e-p and p-p data and it predicts significant suppression of the central-forward jet decorrelations in p-Pb compared to p-p, which we attribute to saturation of gluon density in the nucleus.

PACS numbers: 13.85.Hd

1. Introduction

Nonlinear effects of QCD dynamics are expected to become increasingly important as one goes for a more and more forward production. This is because the forward region corresponds to the density of the incoming gluon being probed at small values of the longitudinal momentum fraction, x , for which a typical k_t of the gluon is of the order of, or smaller than, the saturation scale $Q_s(x)$. To further enhance the relative importance of the saturation region, one may go to the proton-nucleus (p-A) collision as the saturation scale in the nucleus is expected to be significantly higher than in the proton.

The LHC experiments were designed predominantly to measure hard final states like high- p_t jets or vector bosons. The framework that allows one to study dense gluon systems by the means of looking at hard objects is provided by the high energy factorization formalism [1]. In this contribution we show that saturation effects may indeed be observed by looking at the

* Presented at the 42. International Symposium on Multiparticle Dynamics (ISMD), 16-21 September 2012, Kielce, Poland.

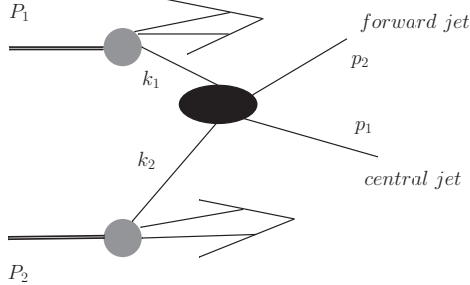


Fig. 1. Jet production in the forward region in hadron-hadron collision.

azimuthal correlations between two leading jets from p-A collisions, one of which is produced in the forward direction. Such a final state probes the parton density of the nucleus at low x , while that of the proton at relatively large longitudinal momentum fraction.

2. High energy factorization

The leading order contribution to dijet production comes from the $2 \rightarrow 2$ partonic process

$$a(k_1) + b(k_2) \rightarrow c(p_1) + d(p_2). \quad (1)$$

The fractions of the longitudinal momenta of the initial state partons are related to the transverse momenta and rapidities of the final state partons by $x_{1,2} = \frac{1}{\sqrt{S}}(p_{t1}e^{\pm y_1} + p_{t2}e^{\pm y_2})$ with S being the squared energy of the incoming hadrons. In the case of forward-central or forward-forward jet production, these fractions of momenta are highly asymmetric, $x_1 \simeq 1$ and $x_2 \ll 1$, we can therefore neglect the transverse momentum of the parton a . Using this fact together with the Sudakov decomposition of 4-momenta of the incoming partons, we arrive at the following formula for dijet production cross section in the high energy factorization approach

$$\frac{d\sigma}{dy_1 dy_2 dp_{t1} dp_{t2} d\Delta\phi} = \sum_{a,c,d} \frac{p_{t1} p_{t2}}{8\pi^2 (x_1 x_2 S)^2} \mathcal{M}_{ag \rightarrow cd} x_1 f_{a/A}(x_1, \mu^2) \phi_{g/B}(x_2, k^2) \frac{1}{1 + \delta_{cd}}, \quad (2)$$

where $k^2 = p_{t1}^2 + p_{t2}^2 + 2p_{t1}p_{t2} \cos \Delta\phi$ and $\Delta\phi$ is the azimuthal distance between the two outgoing partons. All the notation in Eq. (2) corresponds to that in Fig. 1. $\mathcal{M}_{ag \rightarrow cd}$ matrix element for the $2 \rightarrow 2$ process with one off-shell initial state gluon was calculated in [2]. Since the parton a is probed at high values of x_1 , it is legitimate to describe it with the collinear

parton density $f_{a/A}(x_1, \mu^2)$. In our study we used one of the standard pdfs CTEQ6ME [3]. On the other hand, for the incoming gluon, which is probed at small x_2 , we must use the unintegrated gluon density $\phi_{g/B}(x_2, k^2)$, which in addition depends on that gluon's transverse momentum. The sum in Eq. (2) runs over the following sub-processes: $qg \rightarrow qg$, $gg \rightarrow q\bar{q}$ and $gg \rightarrow gg$.

3. Unintegrated gluon distribution in proton and nucleus

In our study, we used the unintegrated gluon density from the unified BK/DGLAP framework [4–6]. This approach provides a well behaved, non-linear gluon distribution inside the proton and it incorporates the main sources of higher order effects. We generalized this framework to the case of a nucleus by assuming the Wood-Saxon nuclear density profile with the nucleus radius given by $R_A = R A^{1/3}$ where R is the proton radius and A is the mass number. In the limit $A \rightarrow 1$ the result for the proton is recovered. The corresponding evolution equation for the distribution of gluons per nucleon in the nucleus A reads

$$\begin{aligned}
\phi(x, k^2) &= \phi^{(0)}(x, k^2) \\
&+ \frac{\alpha_s N_c}{\pi} \int_x^1 \frac{dz}{z} \int_{k_0^2}^{\infty} \frac{dl^2}{l^2} \left\{ \frac{l^2 \phi\left(\frac{x}{z}, l^2\right), \theta\left(\frac{k^2}{z} - l^2\right) - k^2 \phi\left(\frac{x}{z}, k^2\right)}{|l^2 - k^2|} + \frac{k^2 \phi\left(\frac{x}{z}, k^2\right)}{|4l^4 + k^4|^{\frac{1}{2}}} \right\} \\
&+ \frac{\alpha_s}{2\pi k^2} \int_x^1 dz \left[\left(P_{gg}(z) - \frac{2N_c}{z} \right) \int_{k_0^2}^{k^2} dl^2 \phi\left(\frac{x}{z}, l^2\right) + z P_{gq}(z) \Sigma\left(\frac{x}{z}, k^2\right) \right] \\
&- \frac{2A^{1/3} \alpha_s^2}{R^2} \left[\left(\int_{k^2}^{\infty} \frac{dl^2}{l^2} \phi(x, l^2) \right)^2 + \phi(x, k^2) \int_{k^2}^{\infty} \frac{dl^2}{l^2} \ln\left(\frac{l^2}{k^2}\right) \phi(x, l^2) \right], \tag{3}
\end{aligned}$$

where we used the simplified notation: $\phi(x, k^2) \equiv \phi_{g/A}(x, k^2)$ and $\alpha_s \equiv \alpha_s(k^2)$. The second line in Eq. (3) corresponds to the BFKL equation with the kinematic constraint [4] (introduced by the theta function). The third line supplements DGLAP-type corrections and the last line corresponds to the nonlinear term whose strength is enhanced for the nucleus by the factor $A^{1/3}$.

We started off by taking Eq. (3), with an appropriate initial condition, and fitted it to the most recent combined HERA data [7], which allowed us to fix the free parameters of the framework (proton radius R and three other coming from the parametrization of the initial condition). We performed the fit in the kinematical range of $x < 0.01$ and the full range of Q^2 and

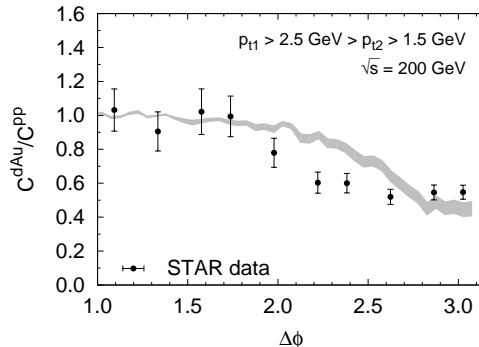


Fig. 2. Ratio of d-Au/p-p coincidence probabilities $C(\Delta\phi)$ for the forward dihadron production at RHIC as a function of the azimuthal distance between the particles. The band corresponds to our prediction with the uncertainty related to unknown yield of uncorrelated dihadron production. For full details see [8].

obtained a very good description of data, with $\chi^2/\text{ndof} = 1.73$. For detailed discussion we refer to [8].

4. Signatures of saturation in dijet production in p-A collisions

Once the framework for the unintegrated gluon density had been fully specified, we used it to study saturation effects in the dijet production in p-A collisions. One observable which is very well suited for studying these effects is the distribution of dijet azimuthal distance $\Delta\phi$. In the region $\Delta\phi \sim \pi$, which corresponds to the two jets being produced almost back-to-back, the gluon density is probed at low k_t where the nonlinear effects are strong and the gluon distribution is expected to be significantly suppressed.

Even though our main focus was on the central-forward dijet production at the LHC, the framework described above allowed us also to make an estimate of the suppression of dihadron production in d-Au collisions at RHIC. Fig. 2 shows the ratio of the normalized π^0 yields in the d-Au and the p-p collisions from STAR [9]. There, we also show our prediction which follows directly from using Eq. (2) together with the unintegrated gluon distribution from Eq. (3) with all the parameters fixed by HERA data and the mass number set to $A=196$ (for detailed procedure see [8]). As we see, our prediction correctly reproduces the suppression observed at RHIC in the region $\Delta\phi \sim \pi$, which shows that our theoretical framework captures the essential physics of this class of processes.

We then moved to the central-forward dijet production in the p-Pb collisions at the LHC. In Fig. 3 we show the corresponding cross section as a function of the azimuthal distance between the jets for two energies of the

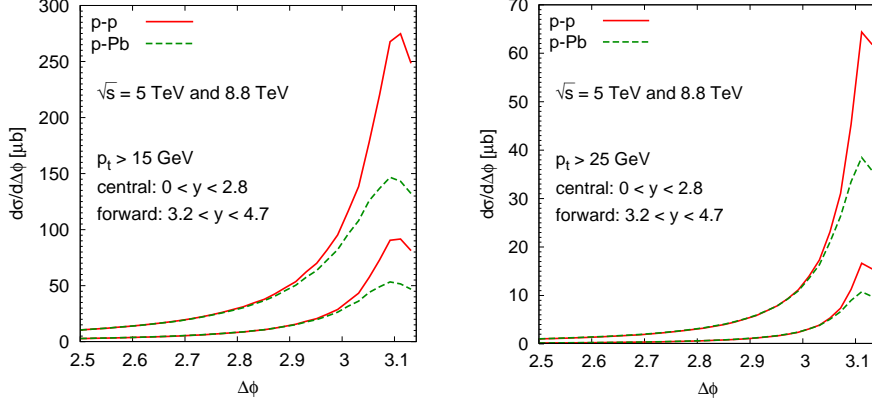


Fig. 3. Differential cross sections for central-forward dijet production at $\sqrt{s} = 5$ TeV and 8.8 TeV as functions of azimuthal distance between the jets $\Delta\phi$ for the case of p-p and p-Pb collisions and two different cuts on jets' p_t .

p-Pb collisions, i.e. the current $\sqrt{s} = 5$ TeV and the nominal $\sqrt{s} = 8.8$ TeV. We also used two different jet p_t cuts 15 and 25 GeV.

We see that the $\Delta\phi$ distribution in the peak region is suppressed by the factor two for the case of the p-Pb collision with respect to p-p, and the effect extends to lower values of $\Delta\phi$ as we lower the jet p_t threshold. This is a consequence of gluon saturation which is stronger in the Pb nucleus than in the proton and leads to suppression of gluon density at low k_t , which is the region probed by the dijet configurations with $\Delta\phi \sim \pi$. As expected, the total yields increase with energy and decrease with p_t cut but the relative difference between the p-p and p-Pb case remains similar.

The distributions shown in Fig. 3 could be subject to further corrections coming from the Sudakov and parton shower effects. They are however expected to act in a similar way for the proton and for the heavy ion collision since they affect the hard scattering. We would like to emphasize that the suppression observed in Fig. 3 comes from the initial state parton density saturation and therefore the relative difference between the cases of p-p and p-Pb will persist even if the very small region near $\Delta\phi = \pi$ may profit from further refinements.

5. Conclusions

We presented predictions for the azimuthal dijet decorrelations in the p-p and p-A collisions in the framework of the high energy factorization with the unintegrated gluon density given by the nonlinear QCD evolution equation. This approach is unique as it allows one to study hard final states in the framework with saturation.

We validated our approach by using HERA F_2 data and we checked that it correctly estimates the suppression of the away side peak observed by STAR. For the LHC, we found that the saturation in the Pb nucleus has a potential to manifest itself as a factor two suppression of the central-forward jet decorrelation in the region of the azimuthal distance between the jets $\Delta\phi \sim \pi$. We argued that this relative difference should be largely insensitive to the final state effects.

Acknowledgments

We thank the organizers of the 42. ISMD conference in Kielce for the very interesting and stimulating meeting. The original results presented here were obtained with Krzysztof Kutak and partially supported by the Foundation for Polish Science with the grant Homing Plus/2010-2/6.

REFERENCES

- [1] S. Catani, M. Ciafaloni, F. Hautmann, Nucl. Phys. **B366** (1991) 135-188.
- [2] M. Deak, F. Hautmann, H. Jung and K. Kutak, JHEP **0909** (2009) 121.
- [3] J. Pumplin, D. R. Stump, J. Huston, H. L. Lai, P. M. Nadolsky and W. K. Tung, JHEP **0207** (2002) 012.
- [4] J. Kwiecinski, A. D. Martin and A. M. Stasto, Phys. Rev. D **56** (1997) 3991.
- [5] K. Kutak and J. Kwiecinski, Eur. Phys. J. C **29** (2003) 521.
- [6] K. Kutak and A. M. Stasto, Eur. Phys. J. C **41** (2005) 343.
- [7] F. D. Aaron *et al.* [H1 and ZEUS Collaboration], JHEP **1001** (2010) 109.
- [8] K. Kutak and S. Sapeta, Phys. Rev. D **86**, **094043** (2012).
- [9] E. Braidot [STAR Collaboration], arXiv:1005.2378 [hep-ph].